Role of the metal–support interface in the total oxidation of carboxylic acids over Ru/CeO_2 catalysts

L. Oliviero, J. Barbier, Jr., S. Labruquère and D. Duprez

Laboratoire de Catalyse en Chimie Organique, UMR6503, CNRS and Université de Poitiers, 40, Av. Recteur Pineau, 86022 Poitiers Cedex, France

Received 1 March 1999; accepted 20 April 1999

Depending on the support morphology and the metal/support contact, Ru/CeO_2 catalysts show very different behavior in catalytic wet air oxidation of acrylic, succinic and acetic acids. TEM and electron diffraction studies favor the hypothesis of a specific role of ceria in oxygen transfer from gas phase to metal sites.

Keywords: catalytic wet air oxidation, carboxylic acids, ruthenium/ceria catalysts

1. Introduction

Wet air oxidation (WAO) is one of the best alternative processes for treating waste water when biological processes are inefficient because of pollutant toxicity or when these pollutants are in too low a concentration for them to be incinerated. Nevertheless, WAO processes require severe reaction conditions (elevated temperatures, 250–350 °C and high pressure, 50–200 bar). Therefore, many efforts have been made to develop catalytic processes (CWAO) to allow operation under milder conditions.

Homogeneous catalysts, Fe [1] or Cu salts [2], were investigated but the additional step required for removing the catalyst from treated water reduces considerably the economic benefit of using a catalytic process. Several heterogeneous processes are now based on the use of noble metal catalysts. In contrast to oxide catalysts (Cu, Zn, Mn, Mn–Ce, etc.) [3–6], they are active and stable in the pH and temperature ranges used in WAO. Hogan et al. investigated the deep oxidation of a large variety of toxic organics in water over Pd/C [7]. Group VIII metals have been shown to be active for wet air oxidation of polyethylene glycol [8,9], phenol [10] and carboxylic acids [10–13]. Ruthenium was one of the most active metals but its activity seemed to depend very much on the nature and the texture of the support [8,13].

The aim of this study was to determine the relationship between metal/support interaction and oxidation activity of Ru/CeO_2 catalysts. Two 5 wt% Ru catalysts supported on ceria (40 and 160 $m^2\,g^{-1}$) were tested in oxidation of various carboxylic acids in the presence of dioxygen. They were characterized by electron microscopy and electron diffraction.

2. Experimental

2.1. Catalyst preparation

Two ceria supports (HSA5, 200 $m^2\,g^{-1}$ and HSA5M, 41 $m^2\,g^{-1}$) provided by Rhodia Rare Earth were used to prepare 5 wt% Ru catalysts by wet impregnation: 9.5 g of the support were stirred slowly for 20 h with an aqueous solution of Ru hexammine chloride (from Alfa) containing 0.5 g of the metal salt. The slurry was dried at 150 °C in air and the catalysts were reduced for 3 h at 350 °C in flowing hydrogen. After thermal treatment, BET areas of supports were 163 $m^2\,g^{-1}$ HSA5 and 41 $m^2\,g^{-1}$ for HSA5M while BET areas of catalysts were 125 $m^2\,g^{-1}$ for Ru/HSA5 and 38 $m^2\,g^{-1}$ for Ru/HSA5M. The catalysts will be herein referred to as Ru/CeO_2 (160) and Ru/CeO_2 (40), respectively.

2.2. Oxidation reactions

Oxidation of various acids (acrylic, succinic and acetic acids) was investigated. These compounds, currently observed as intermediates in CWAO of organic pollutants, were chosen because of their very different oxidability. Aqueous solutions (5 $g\,l^{-1}$ of COD, i.e., 52, 45 and 78 $mmol\,l^{-1}$, respectively, for acrylic, succinic and acetic acids) were prepared from commercial acids (Aldrich, min. 99%) used without any further purification.

Oxidation reactions were carried out at 160 or 200 °C in a 0.5 l Hastelloy C22 autoclave. The initial loading was 160 ml of aqueous solution containing 4 $g\,l^{-1}$ of catalyst and 5 $g\,l^{-1}$ of COD of the pollutant. After heating of the autoclave up to the reaction temperature, pure O_2 was admitted, its partial pressure being maintained at 20 bar for 3 h.

Liquid phase was analyzed by HPLC on an Aminex 87 H column (mobile phase: H_2SO_4 0.004 M; UV detector at a 235 nm wavelength). The chromatograph was calibrated with standard solutions of carboxylic acids in water:

acrylic, succinic, acetic and maleic acids. The gas phase was analyzed by catharometry on a GC equipped with a Porapak Q packed column (1/4 inch, 1 m). Concentration of CO_2 in gas phase was determined by standardization with respect to the O_2 peak, while the carbon dioxide dissolved in water was calculated from a calibration curve giving the concentration of CO_2 in water as a function of its partial pressure in gas phase. These analyses allowed calculation of the percentages of conversion and of mineralization (i.e., the percentage of carboxylic acid oxidized into CO_2) as well as the initial rates in mmol h^{-1} g_{Ru}^{-1}.

2.3. Electron microscopy

Transmission electron microscopy in bright field mode was carried out in a Philips CM120 electron microscope operating at 120 kV with a theoretical resolution of 0.35 nm. The sample was ultrasonically suspended in ethanol, deposited on a Cu grid previously covered with a thin layer of carbon. Selected area electron diffraction patterns were obtained with a beam of 20 nm in diameter.

3. Results

3.1. Oxidation reactions: conversion and mineralization

Acid conversion and carbon dioxide formation versus time were compared for CWAO experiments carried out at 160 or 200 °C. Figure 1 shows the results obtained with succinic acid. Differences between conversion and mineralization indicate that some organic intermediates (acrylic, maleic and acetic acids) are formed and not totally oxidized. Similar results were obtained with the oxidation of acrylic acid which led to acetic acid as an intermediate (table 1), mineralization of acetic acid being totally selective (no organic intermediate). Owing to its C=C double bond, acrylic acid was strongly adsorbed on the catalyst. At 160 °C, the concentrations measured before O_2 admission were 36 mmol l^{-1} with Ru/CeO_2 (160) and 42 mmol l^{-1} with Ru/CeO_2 (40), which corresponds to an adsorption of 4 mmol g^{-1} over Ru/CeO_2 (160) and 2.5 mmol g^{-1} over Ru/CeO_2 (40).

Initial rates of conversion and mineralization are given in table 2 for acrylic, succinic and acetic acids. Whatever the

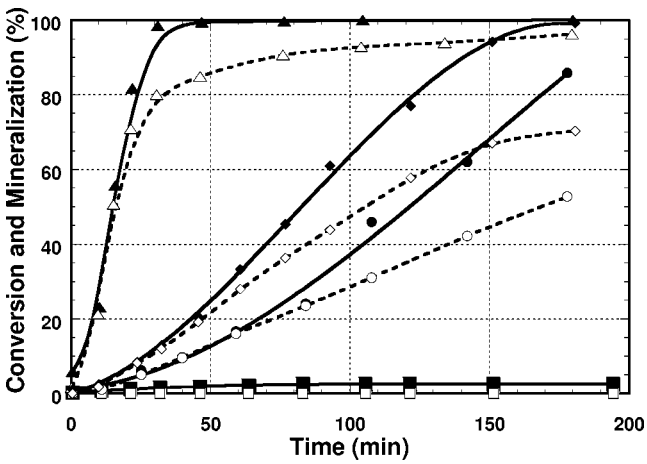

Figure 1. Conversion and mineralization of succinic acid over Ru/CeO_2. Full symbols: conversion; open symbols: mineralization. (□, ■) Blank at 160 °C; (○, ●) Ru/CeO_2 (160) at 160 °C; (◇, ◆) Ru/CeO_2 (40) at 200 °C; and (△, ▲) Ru/CeO_2 (160) at 200 °C.

Table 1
Oxidation of carboxylic acids: percentage of conversion (C%) and mineralization (M%) after 30 min at 160 or 200 °C with and without any catalyst (blank).

Catalyst	Carboxylic acids and reaction temperature					
	Acrylic at 160 °C[a]		Succinic at 200 °C		Acetic at 200 °C	
	C%	M%	C%	M%	C%	M%
Ru/CeO_2 (160)	45	38	97	75	41	41
Ru/CeO_2 (40)	10	6.5	19	11	7	7
Blank	4	0.5	n.d.	n.d.	0.2	0.2

[a] Values calculated with respect to the initial concentration measured after adsorption of acrylic acid.

Table 2
Initial rates of conversion (C) and mineralization (M) of carboxylic acids over Ru/CeO_2 (160) and Ru/CeO_2 (40). The selectivity to CO_2 (Sel.%) corresponds to the M to C ratio.

Acid	T (°C)	Initial rate (mmol h^{-1} g_{Ru}^{-1})					
		Ru/CeO_2 (160)			Ru/CeO_2 (40)		
		C	M	Sel.%	C	M	Sel.%
Acrylic	160	252	216	85.7	49	30	61.2
	200	488	394	80.7	–	–	–
Succinic	160	60	22	36.7	–	–	–
	200	480	239	49.8	110	33	30
Acetic	160	30	30	100	–	–	–
	200	380	380	100	74	74	100

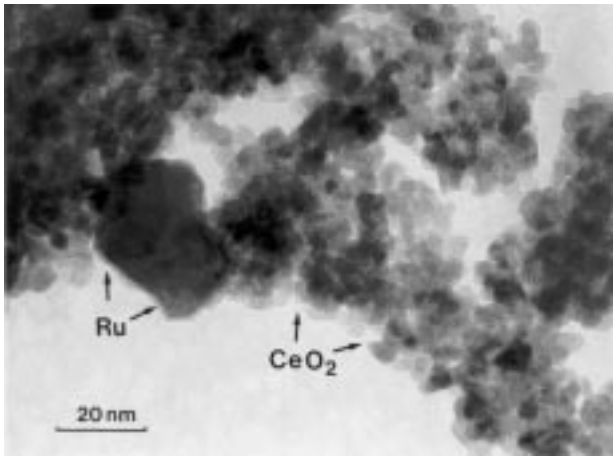

Figure 2. TEM picture of Ru/CeO_2 (160).

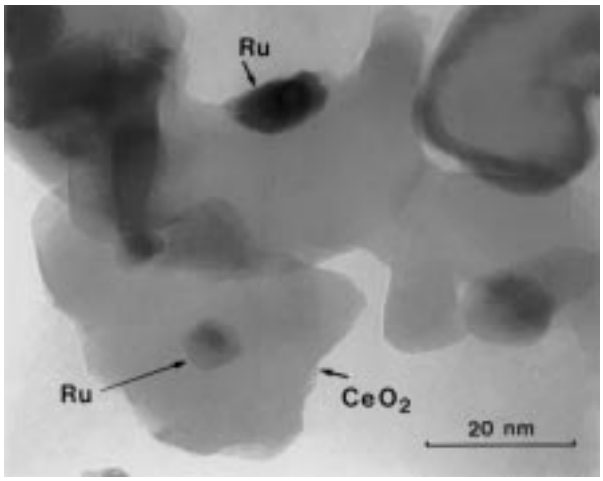

Figure 3. TEM picture of Ru/CeO_2 (40).

acid or the reaction temperature, Ru/CeO_2 (160) is about five times more active than Ru/CeO_2 (40). Moreover, for acrylic and succinic acids, the mineralization is favored on the high surface area catalyst.

3.2. Characterization of catalysts

The two Ru/CeO_2 were characterized by electron microscopy and electron diffraction to understand why they behave differently in oxidation.

About 100 particles were examined by TEM. A certain number of these particles are shown in figures 2 (Ru/CeO_2 (160)) and 3 (Ru/CeO_2 (40)). Large Ru particles of homogeneous size (20–30 nm) can be seen on the catalyst prepared with the high surface area support. Each metal particle is surrounded by small clusters of ceria of about 7 nm. Electron diffraction patterns of several Ru particles were obtained on the Ru/CeO_2 (160) sample. As already proved by XRD [13], these diffraction patterns confirm that Ru remains in the metallic state after reaction (figure 4). Moreover, the same crystallographic orientation can be observed, all the particles growing along the $(\bar{1}11)$ axis. A very different morphology can be observed for

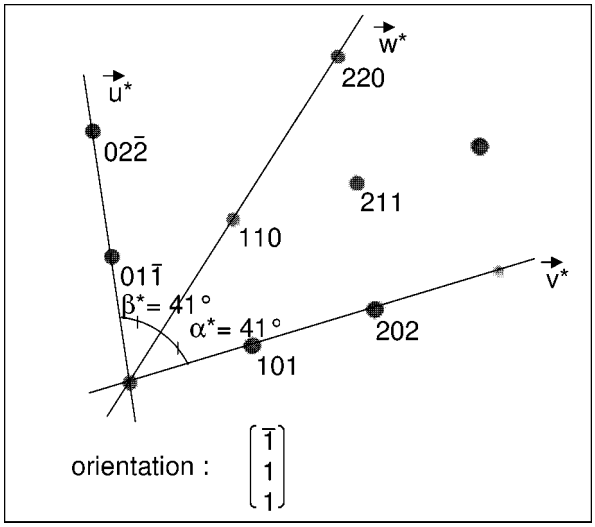

Figure 4. Electron diffraction pattern of a Ru particle recorded on Ru/CeO_2 (160) catalyst.

Ru/CeO_2 (40) (figure 3). Unexpectedly, Ru particles here are smaller (8–12 nm) than in Ru/CeO_2 (160) and in close contact with relatively large CeO_2 particles (about 25 nm). In contrast to what is observed in Ru/CeO_2 (160), various crystalline orientations of Ru particles can be noticed in Ru/CeO_2 (40), corresponding to particles growing preferentially along $(1\bar{3}1)$ and (010) axes (see figure 5). Rarely has the $(\bar{1}11)$ orientation of Ru particles been observed on Ru/CeO_2 (40).

4. Discussion

Modelling of the metal/support interaction

We consider that the significant difference of activity between the two catalysts can be correlated with their structure which we observed by TEM.

First, the particle size of Ru may be expected to play a role in the oxidation reaction. Previous studies [12,13] have shown that oxidation of acetic acid is a reaction sensitive to the metal particle size. However, the decrease of the ruthenium metal area was compensated by an increase of the turnover frequency so that the specific activity (per gram of catalyst) was almost constant within the 7–57% dispersion range [13]. Therefore, the difference in the particle sizes of Ru cannot account for the low activity of Ru/CeO_2 (40).

As pointed out by Trovarelli [14] and by Imamura et al. [15], the metal–ceria interaction is a key factor in controlling the catalyst performance, particularly in oxidation reactions. TEM pictures (figures 2 and 3) show that the catalysts Ru/CeO_2 (160) and Ru/CeO_2 (40) present a totally different morphology of their metal/support interface, which is schematized on figure 6.

Assuming a spherical shape for the ceria particles, a theoretical diameter of 6.8 nm for Ru/CeO_2 (160) and of 22 nm for Ru/CeO_2 (40) can be calculated from BET area of ce-

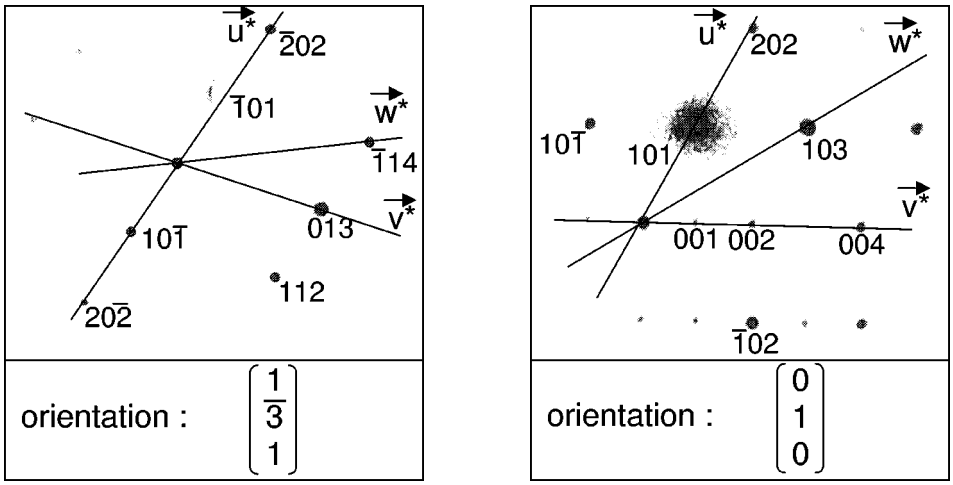

Figure 5. Electron diffraction patterns of Ru particles recorded on Ru/CeO_2 (40) catalyst.

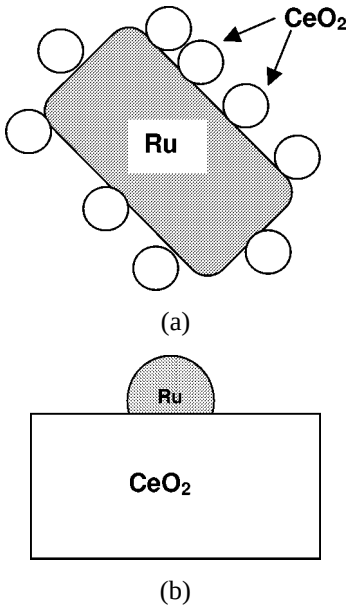

Figure 6. Schemes of the metal/support interface: (a) Ru/CeO_2 (160) and (b) Ru/CeO_2 (40).

ria. These values are very close to those of the particle size of ceria determined by TEM (7 and 25 nm, respectively). This proves that virtually the ceria particles are not microporous. They are constituted of nanocrystals of fluorite structure, which was confirmed by electron diffraction taken on several particles (diffraction patterns not shown).

On the basis of the actual weight percentage of Ru (5%) and the specific weights of Ru (12.30 $g\,cm^{-3}$) and CeO_2 (7.13 $g\,cm^{-3}$), the number n of particles of ceria per particle of ruthenium is

$$n = 32.8\left(\frac{d_{\mathrm{Ru}}}{d_{\mathrm{Ce}}}\right)^3. \qquad (1)$$

Equation (1) shows that, in the Ru/CeO_2 (160) catalyst, each metal particle is surrounded with 1620 particles of ceria. As shown by TEM (figure 2), this number is much greater than the number n_{C} of CeO_2 particles which can be in direct contact with the metal. Assuming a cubic stacking of nanospheres of ceria all around a Ru particle, the maximal value of n_{C} would be

$$n_{\mathrm{C}} = 6\left(\frac{d_{\mathrm{Ru}} + d_{\mathrm{Ce}}}{d_{\mathrm{Ce}}}\right)^2, \qquad (2)$$

which shows that about 130 particles of ceria can be in direct contact with Ru. In this model, CeO_2 spheres are in contact with a ruthenium surface and we can assume that each contact point is constituted of at least 6 Ru atoms. For each metal particle, 780 Ru atoms would be in direct contact with ceria, i.e., 0.21 Ru atom nm_{Ru}^{-2}.

The morphology of Ru/CeO_2 (40) is quite different since this catalyst is constituted of Ru particles of about 10 nm supported on large particles of ceria. Equation (1) leads to $n = 10$, which means that one particle of ceria out of ten is covered with Ru. In the case of Ru/CeO_2 (40), the Ru atoms in contact with ceria are located at the metal/support interface, on a line corresponding to the particle perimeter. The mean distance between Ru atoms being 0.25 nm, there would be, per metal particle, about 125 Ru atoms in contact with ceria, i.e., 0.21 Ru atom nm_{Ru}^{-2}.

The two Ru/CeO_2 catalysts have practically the same surface density of Ru atoms in direct contact with ceria. Nevertheless, these atoms on Ru/CeO_2 (40) are concentrated on the particle periphery while, in Ru/CeO_2 (160), they are regularly distributed all around the metal particle. As carboxylic acids are more strongly adsorbed than oxygen over noble metals [13,16], the better distribution of Ru–Ce pairs at the surface of Ru/CeO_2 (160) can accelerate the oxygen transfer from gas phase to the metal sites. Similar effects have been found in CO oxidation over noble metals which is generally limited by O_2 adsorption. The noble metal is essentially covered with CO which reacts with oxygen from ceria at the metal/support interface: ceria increases the reaction rate, particularly at low O_2/CO ratio [17–21].

Lastly, electron diffraction has shown that ceria had a specific role on growth and orientation of Ru. The ruthenium planes, systematically observed along the ($\bar{1}11$) growth axis in Ru/CeO_2 (160), seem to offer a better configuration for adsorption of carboxylic acid and oxygen than the other Ru planes observed in Ru/CeO_2 (40). This point requires further theoretical studies which are in progress.

5. Conclusion

The kinetic results obtained in wet air oxidation over Ru/CeO_2 catalysts are coherent with a limiting step of oxygen transfer from gas phase to metal sites. This is the case for oxidation of carboxylic acids which are more strongly adsorbed than O_2 on the metal. CeO_2, able to favor oxygen transfer and to promote specific metal–support interaction, is very interesting in CWAO applications. The best performances are obtained with high surface area ceria, which leads to a specific morphology of catalyst: large crystallites of Ru ($\sim$25 nm), all of them being oriented along a ($\bar{1}11$) axis, are surrounded with small particles of ceria ($\sim$7 nm) allowing a fast oxygen transfer.

Acknowledgement

Thanks are due to Aurélie Bacle and Marie Rémondière for their technical assistance.

References

[1] A.K. Chowdhury and L.W. Ross, AIChE Symp. Ser. 151 (1975) 46.
[2] S. Imamura and K. Okuda, J. Techn. Water Treatment Jpn. 22 (1981) 201.
[3] A. Pintar, J. Batista and J. Levec, in: *Proc. 1st World Conf. Environmental Catalysis*, Pisa, Italy, eds. G. Centi et al. (1995) p. 491.
[4] S. Imamura, H. Nishimura and S. Ishida, Sekiyu Gakkaishi 30 (1987) 199.
[5] F. Luck, M. Djafer and M.M. Bourbigot, Catal. Today 24 (1995) 73.
[6] A. Fortuny, J. Font and A. Fabregat, Appl. Catal. B 19 (1998) 165.
[7] T. Hogan, R. Simpson, M. Lin and A. Sen, Catal. Lett. 40 (1996) 95.
[8] S. Imamura, I. Fukuda and S. Ishida, Ind. Eng. Chem. Res. 27 (1988) 721.
[9] D. Mantzavinos, R. Hellenbrand, A.G. Livingston and I.S. Metcalfe, Appl. Catal. B 11 (1996) 99.
[10] D. Duprez, F. Delanoë, J. Barbier, Jr., P. Isnard and G. Blanchard, Catal. Today 29 (1996) 317.
[11] P. Gallezot, N. Laurain and P. Isnard, Appl. Catal. B 9 (1996) 11.
[12] P. Gallezot, S. Chaumet, A. Perrard and P. Isnard, J. Catal. 168 (1997) 104.
[13] J. Barbier, Jr., F. Delanoë, F. Jabouille, D. Duprez, G. Blanchard and P. Isnard, J. Catal. 177 (1998) 378.
[14] A. Trovarelli, Catal. Rev. Sci. Eng. 38 (1996) 439.
[15] S. Imamura, Y. Okumura, T. Nishio and K. Utani, Ind. Eng. Chem. Res. 37 (1998) 1136.
[16] J.C. Béziat, M. Besson, P. Gallezot, S. Juif and S. Durécu, Stud. Surf. Sci. Catal. 110 (1997) 615.
[17] S.H. Oh and C.C. Eickel, J. Catal. 112 (1988) 543.
[18] C. Serre, F. Garin, G. Belot and G. Maire, J. Catal. 141 (1993) 9.
[19] G.S. Zafiris and R.J. Gorte, J. Catal. 143 (1993) 86.
[20] T. Bunluesin, E.S. Purna and R.J. Gorte, Catal. Lett. 41 (1996) 1.
[21] R.H. Nibbelke, M.A.J. Campman, J.H.B.J. Hoebink and G.B. Marin, J. Catal. 171 (1997) 358.